Journal of Engineering Science and Technology Review 16 (4) (2023) 119 - 126

Research Article

JOURNAL OF
Engineering Science and Technology Review

www.jestr.org

Study on Tea Identification of Hyperspectral Image Integrating Spectral and Texture Features

Qingkong Cai [1,*], Erjun Li[2], Youpeng Tao[1], Guo Wang[1] and Li Liu[3]

[1]*College of Civil Engineering, Henan Universsity of Engineering, Zhengzhou 451191, China*
[2]*College of Human and Social Sciences, Henan Universsity of Engineering, Zhengzhou 451191, China*
[3]*School of Social Sciences, University Sains Malaysia, Penang 11800, Malaysia*

Received 7 June 2023; Accepted 20 August 2023

Abstract

The category identification and grade classification of tea are important to food safety and life safety. The category and grade of the whole tea batch are typically determined by random sampling. However, full distribution graphs of tea categories are hardly available. This study analyzed relevant features and model construction to improve model precision for the category identification of tea. Moreover, spectral and texture features of hyperspectral images of tea were discussed through principal component analysis and gray level concurrence matrix. The category identification models of tea based on spectral features, texture features, and the integration of the two were constructed on the basis of the support vector machine model. The optimal model was applied to hyperspectral images to produce the full category distribution graph of tea. Then, its accuracy was verified through an assessment. Results demonstrate that the model based on hyperspectral images integrating spectral and texture features achieves the highest accuracyon the prediction set, and the total accuracy reaches 94.3%. This outcome is higher than the accuracy of the model based on spectral features (88.9%) and the model based on texture features (85%). On the full-image scale, the overall classification accuracy of the model based on hyperspectral images of four kinds of tea reaches 90.3% when the training sample is only 1%. In addition, the corresponding Kappa coefficient is 0.87, indicating that the established model is feasible. The integration of spectral and texture features can overcome the influences of having different spectra for the same object to some extent. The proposed algorithm provides scientific guidance for authenticity verification, grade classification, and other practical production of tea.

Keywords: Hyperspectral image, Texture features, Spectral features, Category identification, Tea

1. Introduction

Food safety determines life safety and social safety. During the "13th Five-year Plan," food safety prioritized as a national great strategy [1]. The internal and external qualities of tea, including color, appearance, taste, and fragrance, directly determine its grade. Nevertheless, the tea market has experienced regulation issues, such as selling seconds at the best quality price as well as fake and poor-quality commodities. All of these factors seriously hinder the development of the tea industry. Hence, the quality and category identification of tea have become crucial. The sensory ranking method and electronic nose technology are major traditional methods to identify tea categories [2]. These methods are time consuming, labor consuming, and economically inefficient. Hence, they cannot evaluate the quality of tea objectively and quickly. Compared with traditional methods, hyperspectral imaging can acquire internal structural features and external information of testing substances. Moreover, it is a fast nondestructive testing technology [3,4].

Existing category identification mainly includes category identification based on spectral technology, category identification based on image processing technology, and category identification based on hyperspectral images [5-7]. The former two are mainly limited to the use of partial spectral or image information. On the one hand, a disturbance of external factors (e.g., sampling position, sampling time, and illumination of plants) exists in the spectral information collected by a spectrometer. On the other hand, the category identification method based on image processing technology underuses spectral information and can only provide limited feature spaces. Thus, identifying category information upon the influences of multiple factors becomes difficult. These methods fail to evaluate the internal and external qualities of tea comprehensively and leave a great gap with practical applications. Imaging spectrometry has remarkable advantages for category identification because it integrates traditional spectral technology and computer image technology. Furthermore, it breaks many limits of visible multispectral images. However, most existing studies generally judge the quality of batches through a limited number of samples. Further studies on full category distribution graphs based on imaging spectral data are still needed.

Therefore, the dimensions of the hyperspectral images of the four kinds of tea were reduced by principal component analysis (PCA) to extract their spectral features. The texture features of tea were extracted on the basis of the gray level concurrence matrix method (GLCM). A tea quality identification model was built by combining a support vector machine (SVM). The research conclusions can provide some technological support for practical production detection.

*E-mail address: hnnzcqk@163.com
ISSN: 1791-2377
doi:10.25103/jestr.164.15

2. State of the art

Hyperspectra can capture reflectance at a very high spectral resolution after electromagnetic waves act on substances. Many studies have identified categories through nonimaging spectral technology. For instance, Kos et al. [8] distinguished mildew peanuts and corn samples using mid-infrared spectroscopy. In addition, Fu et al. [9] identified mildew pollution of sunflower and soybean using near-infrared spectroscopy. Huang et al. [10] collected near-infrared (NIR) spectral data of mung beans in the shape of particles and powder in cold northern China. A nondestructive detection method of the origin of mung beans was established by screening the wavenumber of NIR spectral features. Meanwhile, Chen et al. [11] established a detection method for the origin of Lonicera japonica using NIR spectral technology and partial least squares discriminant analysis. Liu et al. [12] extracted the feature wavebands of full-band spectra of Xinjiang jujubes by combining hyperspectral technology and machine learning algorithms. Then, they established a model based on feature wavebands. The results proved that the established model had very high identification accuracy. Li et al. [13] proposed a fast nondestructive identification technique for green tea based on NIR and chemometrics by scanning and obtaining NIR spectra.

The above studies of category identification based on spectral technology only use spectral information without the involvement of image information. Disturbances of external factors (e.g., sampling position, sampling time and illumination of plants) exist in the information collected by a spectrometer. On this basis, some scholars have studied category identification using image processing technology. By combining digital image processing technology and machine learning, Zhang [14] proposed an image identification technique of tea based on the K-means and SVM coupling algorithm according to different colors between high-quality and poor-quality tea particles. Chaitra et al. [15] believed that the red waveband (R) in RGB channels of visible light has good separability of mildew peanuts; thus, they proposed an identification method of mildew peanuts based on "color mapping" by using this waveband. Furthermore, Liu et al. [16] identified and deleted damaged soybean seeds on the basis of image features and constructed a classification model using a series of image processing algorithms, such as data fusion and morphological corrosion expansion. Through examining tea images under natural conditions, Wang et al. [17] realized the automatic identification and segmentation of tea shoots using digital image processing technology. However, the above studies mainly identify product categories on the basis of RGB images and machine vision. RGB can provide very limited spectral information and can only use information of image tones, textures, and shapes. Few studies have concentrated on category identification that integrates spectra and image texture information.

Imaging spectral technology shows remarkable advantages in tea for "image-spectra integration" and supply of spectral and image spatial information at the same time. Studies on applications of hyperspectral imaging technology to tea are mainly divided as follows: (1) growth monitoring and pest monitoring in the planting and management process [18-21], (2) inversion of quantitative indexes and qualitative evaluation of tea during production and processing [22,23], and (3) tea identification. This technology can not only identify different kinds of tea but also detect the degree of adulteration [24]. Kelman et al. [25] classified five kinds of tea through maximum likelihood and artificial neural networks and provided classification images to present identification results intuitively. In addition, Wang et al. [26] classified and identified inoculated corn kernels using 400-1000 nm and 1000-2500 nm hyperspectral images by combining PCA and factor discriminant analysis. The classification accuracy of the five levels reached more than 88%. Furthermore, Rabanera et al. [27] predicted the water content in peanuts by combining 900-1700 nm NIR hyperspectral images and PLSR. The decision coefficient of their test set was 0.94. Moreover, the visual distribution of water content in peanuts was determined, which provided references for the judgment of peanut quality and storage stability. Qiao et al. [28] identified multiple categories of mildew peanuts by combining pattern recognition and spatial image segmentation, thus obtaining relatively satisfying results. Moreover, Singh et al. [29] constructed a model on the basis of average spectra and a one-dimensional convolutional neural network by using hyperspectral technology; this model was then used to classify different categories of barley seeds. At present, research on category identification using hyperspectral image technology has the following shortcomings. Most studies are based on samples but do not give full distribution graphs of tea categories. Moreover, research results are influenced by the imaging environment and shapes of samples. Evident phenomena of having different spectra for the same object occur. Hence, extracting spectral features from hyperspectral data under the influences of having different spectra for the same object and generating full category distribution graphs must be further studied.

On the basis of the above analysis, this work established a method to identify string-shaped teas with similar appearances using hyperspectral images. This method can address the following questions. How can robust spectral features and texture features be extracted for category identification under the influences of having different spectra for the same object? How can a high-precision tea identification model be built and full category distribution graphs of tea be given?

The remainder of this study is organized as follows. Section 3 describes the acquisition and preprocessing of tea sample materials and hyperspectral image data, as well as the research method during the construction of tea identification models. Section 4 extracts the spectral features and texture features of tea by analyzing the spectral response features of tea. A tea identification model is built, and full category distribution graphs of tea are generated. Section 5 summarizes the conclusions.

3. Methodology

3.1 Acquisition of tea sample materials

Tea sample materials were bought randomly from a tea shop in Xingfu Supermarket at Xueyuan Road, Haidian District, Beijing. In this study, four types of string-shaped tea with similar appearances were selected, namely, Junshan Yinzhen Tea, Wuxi White Tea, Xinyang Maojian Tea, and Lu'an Guapian Tea. Each kind of tea was purchased in a volume of 250 g. Meanwhile, chippings and suspicious impurities were removed manually to assure the uniformity of tea samples.

3.2 Acquisition of hyperspectral image data

The hyperspectral data acquisition system is composed of an ImSpector N25E hyperspectral imager, a light source system, and a mechanical drive system. First, the four kinds of tea samples were placed on the black cloth of the mechanical transfer platform, which moved at a constant speed upon driving by the motor. A tungsten light source irradiated the tea samples. The reflected lights of tea samples were captured by the camera through a lens, thus obtaining spectral data of pixels on the column of scanning seams of the imaging spectrometer. As the transfer platform moved at a constant speed, hyperspectral images of all tea samples were acquired through push scanning. For the acquired hyperspectral images, the spectral range, spectral resolution, number of pixels per row, and number of wavebands were 1000–2500 nm, 6.30 nm, 320 and 239, respectively. The imaging mode used was push-scanning.

3.3 Preprocessing of hyperspectral image data

3.3.1 Radiation correction

During scanning imaging, the reflectance of the reference white board and black board as well as dark current data were acquired except for the hyperspectral images of tea. These data can help realize the radiation correction of hyperspectral images of tea. Later, the DN value of the original hyperspectral data can be transformed into reflectance. The specific radiation correction is expressed as follows [30]:

$$R = \frac{I_S - I_D}{I_W - I_D} \times 100\% \tag{1}$$

where R is the relative reflectance of the corrected hyperspectral image, $R \in [0,100]$. I_S is the DN value of the original hyperspectra of tea. I_D is the DN value of the dark current image. I_W is the DN value of the calibration images of the reference board.

3.3.2 Spectral smoothing

Given the system error of the imaging spectrometer, the influences of dark spot flows, and the inconsistent influences of noise on different wavebands, noise is inevitable in hyperspectral images. Hence, spectral smoothing is essential to eliminate high-frequency random error during the spectral sampling process. As a result, a five-point moving mean smoothing method was applied to hyperspectral images [31]. This method is expressed as:

$$R_S = \frac{1}{2.5}\left(\frac{1}{4}R_{i-2} + \frac{1}{2}R_{i-1} + R_i + \frac{1}{2}R_{i+1} + \frac{1}{4}R_{i+2}\right) \tag{2}$$

where R_S is the spectra after smoothing of each pixel. R_i is the reflectance of waveband i, $i \in [3, k-2]$, where k is the number of wavebands of hyperspectral images.

After smoothing the hyperspectral images, these wavebands were deleted selectively because of the low signal-to-noise ratio of channels at two ends of the spectral range as well as signal mutation in some wavebands. Finally, 230 wavebands were retained for subsequent treatment. Moreover, the background of tea was masked. This masking determines the segmentation threshold according to the gray level history of wavebands and features. Finally, the hyperspectral images of four kinds of tea were acquired. A total of 250 samples were selected randomly for each kind of tea on images using region of interest (ROI), thus summing to 1,000 samples. Among them, 700 samples were chosen randomly as the training set of the model. The remaining 300 samples were used as the test set.

3.4 Principal component analysis

PCA [32,33], also called Hotelling transformation, is mainly used to map n-dimensional features onto *k*-dimensional features. These *k*-dimensional features are fresh new orthogonal features or principal components. These features were rebuilt on the basis of the original *n*-dimensional features. The principal components can be formed by a linear combination of images under different wavebands:

$$PC_j = \sum_{i=1}^{n} \alpha_i I_i \tag{3}$$

where PC_j is the image of the *j*th principal component. I_i is the gray image corresponding to the *i*th waveband. α_i is the weight coefficient of I_i in PC_j. After Eq.(3) is unfolded, the image under the wavelength corresponding to the maximum weight absolute (α_i) has the maximum contribution to PC_j .After component transformation, principal components are unrelated, and the information size decreases with the increasing principal component number. Given that the principal components that rank the back positions contain a very small amount of information, they can be viewed as noise. Hence, PCA can concentrate redundant information contained by multivariable data into a few principal components. This approach is highly effective with respect to the big data size of hyperspectral images as well as the strong correlation and information redundancy among adjacent wavebands. In this study, PCA was applied for the dimension reduction of hyperspectral data.

3.5 Gray level concurrence matrix

The GLCM [34,35] usually analyzes texture features of gray images with references to pixel gray and positional information. It analyzes the gray combination of any point in the image space with pixels in the adjacent zone with some distances. The GLCM is defined as the probability $P(i,j,d,\theta)$or the pixel $(m,n)$with a gray level of i to leave a fixed point distance $(d)$to the pixel with a gray level of $j(m+a,n+b)$. All estimated values can be expressed as a matrix:

$$P(i,j,d,\theta) = \left[(m,n) \quad (m+a,n+b) \quad f(m,n) \quad f(m+a,n+b)\right] \tag{4}$$

where $\theta$is the direction of generation of the GLCM, which is usually one of the four directions of 0°, 45°, 90°, and 135°. $f(.)$is the grayscale calculation function. Mean, variance, standard deviation, homogeneity, contrast, dissimilarity, entropy, and correlation are major common feature statistical indexes that are used to extract texture information in remote sensing images.

3.6 Support vector machine model

The tea categories were identified using a support vector machine (SVM) [36]. This model is a support vector library developed by Professor Lin Zhiren from Taiwan. It is

applicable to the linear or nonlinear classification of high-dimensional spatial problems as well as the detection of regression and outlier points. SVM is a machine learning model algorithm based on statistical theory that maps low-dimensional spatial vectors onto high-dimensional spatial vectors. Based on optimization solving, the optimal classification hyperplane is determined in the high-dimensional feature space of the data. Hence, it achieves a series of advantages, such as minimum classification error, improved generalization ability of the classifier to the maximum extent, good robustness and expansion, and processing of large-scale data. Given these advantages, SVM has been widely applied to classification problems. The optimal classification function of SVM is:

$$f(x)=sign\left[\sum_{i=1}^{n}a_i^*y_iK(x,x_i)+b^*\right] \tag{5}$$

where a_i^* and b^* are the optimal solutions obtained by convex quadratic programming; y_i is the category symbol; $K(x,x_i)$ is the kernel function, x and x_i are the vectors to be classified and the support vector, respectively.

At present, SVM has four common types of kernel functions, including the sigmoid kernel function, polynomial kernel function, radial basis function (RBF), and linear kernel function (Linear). Specifically, RBF was used as the kernel function:

$$K(x,x_i)=\exp\left(-\frac{\|x-x_i\|^2}{2\sigma^2}\right),\sigma>0 \tag{6}$$

where σ is the Gaussian kernel bandwidth.

4. Result Analysis and Discussion

4.1 Spectral features of different tea categories

To understanding the spectral response differences of tea, 10 pixels were randomly selected for each kind of tea. The four kinds of tea were expressed by red, green, blue, and yellow (Fig. 1).

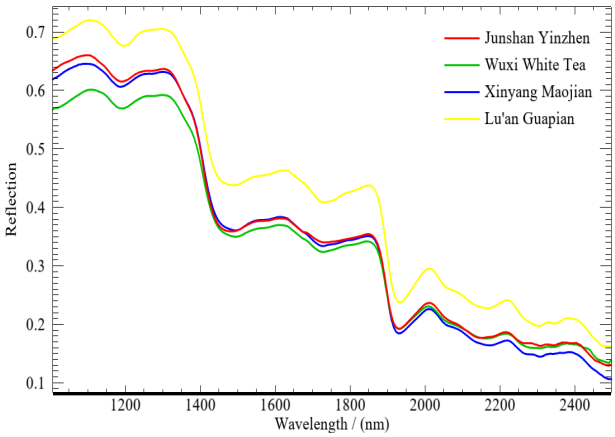

Fig. 1. Spectral curves of four kinds of tea.

4.2 Extraction of spectral and texture features of tea

4.2.1 Extraction of spectral features of tea

The PCA of hyperspectral images was conducted, and the results are shown in Table 1. Clearly, the cumulative variance contribution rate of the first three principal components reached 99.94%. They covered most of the information of the original waveband data and could explain most of the information of the original hyperspectral images. Hence, the images of the first three principal components were extracted as spectral features of tea (Fig. 2).

Table 1. PCA of hyperspectral images of tea

Principal components	Feature value	Contribution rate	Cumulative contribution rate
PC1	6.0967	97.93%	97.93%
PC2	0.1162	1.87%	99.80%
PC3	0.0086	0.14%	99.94%

4.2.2 Extraction of texture features of tea

After the PCA of hyperspectral images, the first three principal components could sufficiently interpret 99.94% of the information of the original images. In addition, they could interpret most of the information of the original hyperspectral images. Hence, the images of PC2 began to develop noise information. The feature waveband image was searched using the images of PC1. According to the principle of PCA, images of different principal components are formed by linear combination of images of different wavebands. The image under the wavelength corresponding to the maximum absolute weight coefficient makes the largest contribution to the principal components, which is known as the feature image [37]. The weight coefficients at waveband 17 (1107.01 nm) and waveband 46 (1289.43 nm) were the highest in the images of PC1. Hence, these two wavebands were selected as feature wavelengths to analyze texture. Waveband 17 (1107.01 nm) and waveband 46 (1289.43 nm) are shown in Fig. 3.

The GLCM calculation of wavebands 17 and 46 of the hyperspectral images obtained eight texture features of hyperspectral images, namely, mean, variance, Std, homogeneity, contrast, dissimilarity, entropy, and correlation. A total of 16 texture feature images were obtained for two wavebands. The texture features of waveband 17 of Junshan Yinzhen Tea are shown in Fig. 4.

4.3 Construction of models

4.3.1 Construction of the model based on spectral features

The images of three principal components were extracted through PCA. Combined with the selected ROI sampling points, the training samples of the four tea categories were extracted and input into the dataset. The classification values of the four categories were defined as 1, 2, 3, and 4. The tea classification values were extracted by ROI sampling points and used as the output dataset of the model training samples. Then, they were input into the SVM classifier. In addition, RBF was chosen as the kernel function. The penalty coefficient and kernel parameter in the SVM classification model were acquired by cross validation [38]. A tea identification model based on spectral features was constructed.

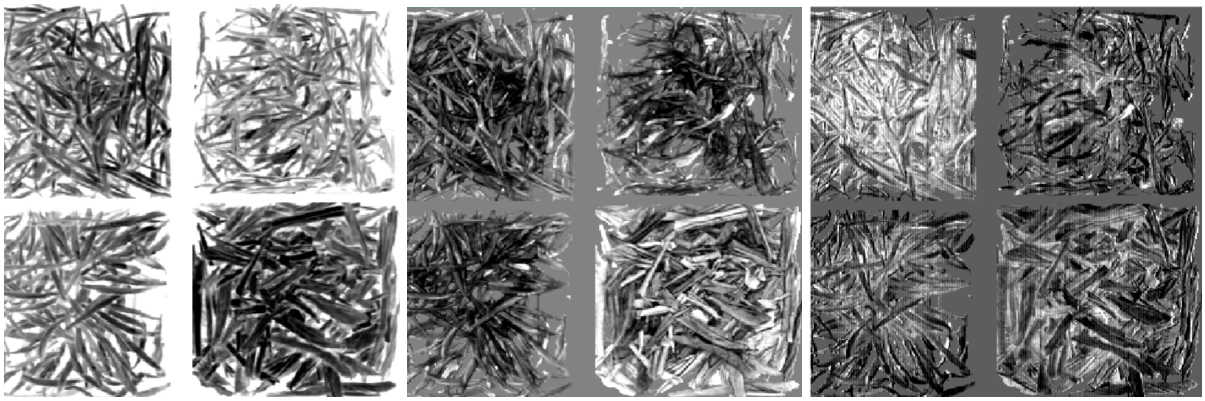

(a) (b) (c)

Fig. 2. Clustering result for the karate network. (a) PC1. (b) PC2. (c) PC3

(a) (b)

Fig. 3. Feature images extracted by PCA. (a) b17. (b) b46

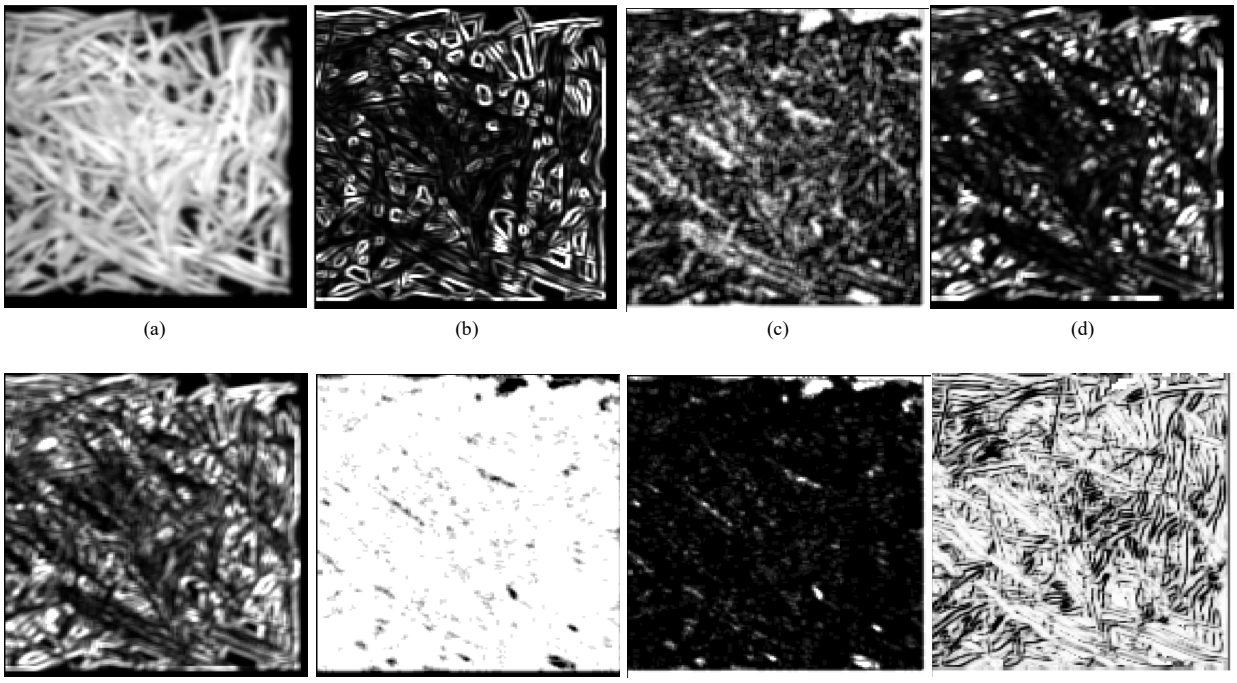

(a) (b) (c) (d)

(e) (f) (g) (h)

Fig. 4. Tea texture feature image of band17. (a) Mean. (b) Variance. (c) Std. (d) Homogeneity. (e) Contrast. (f) Dissimilarity. (g) Entropy. (h) Correlation

4.3.2 Construction of the model based on texture features

The images of 16 texture features extracted by wavebands 17 and 46 as well as the selected ROI sampling points were used to extract the training samples of the four tea categories. Then, these samples were input into the dataset and were used as variables of texture features. The classification values of the tea categories extracted by ROI sampling points were used as the output dataset of the model training samples. They were input into the SVM classifier to train the SVM model. In addition, RBF was selected as the kernel function. The penalty coefficient and kernel parameter in the SVM classification model were acquired by cross validation. A tea identification model based on texture features was constructed.

4.3.3 Construction of the model based on spectral and texture features

The three spectral features in Section 4.3.1 and 16 texture features in Section 4.3.2 were used as the input dataset of the training samples. The classification values of the four tea categories extracted by ROI sampling points were used as the output dataset of the model training samples. They were input into the SVM classifier. RBF was selected as the kernel function. The penalty coefficient and kernel parameter in the SVM classification model were acquired by cross validation. Then, all residual pixels were classified. A tea identification model based on spectral and texture features was constructed.

4.3.4 Accuracy evaluation of the model

After the models were constructed, 300 prediction set samples were input into three models to calculate their total accuracy values. The model based on texture and spectral features achieved the highest accuracy with a total accuracy of 94.3%. Meanwhile, the model based on spectral features achieved the second highest accuracy (88.9%). In addition, the model based on texture features had the lowest accuracy (85%). Hence, four kinds of tea were classified through the model on the basis of texture and spectral features. The results are shown in Fig. 5. Moreover, a statistical analysis of the image pixel classification results of the four tea categories conducted. Pixel statistics and classification accuracy are listed in Table 2.

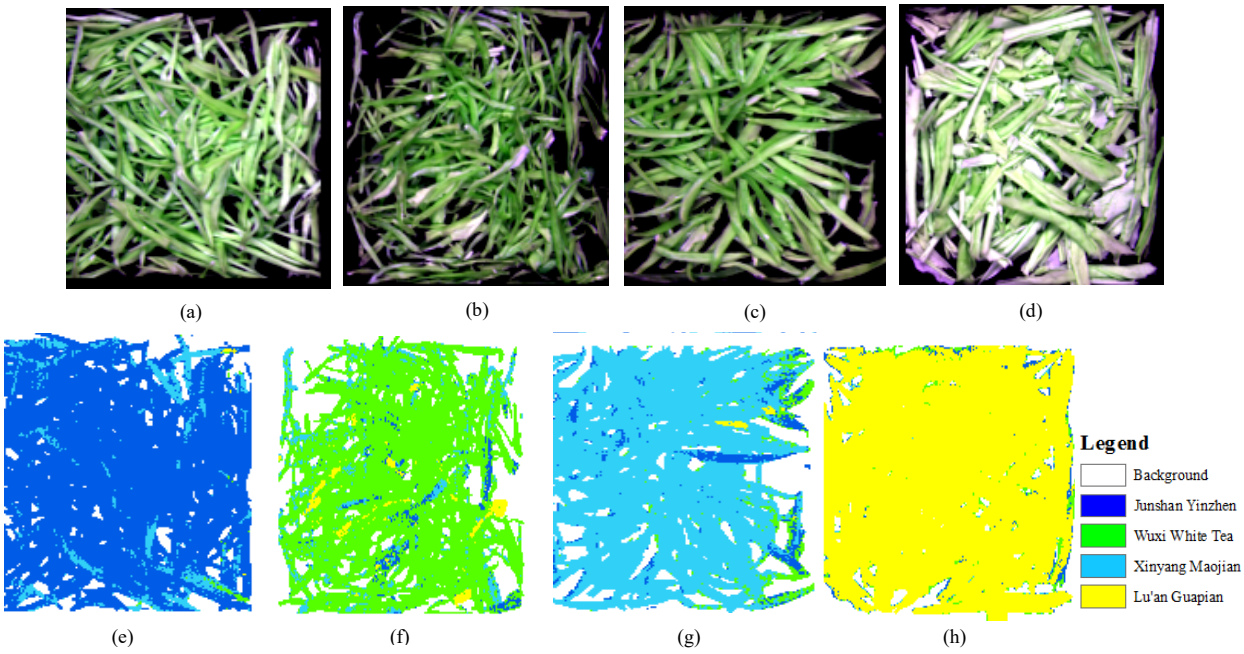

Fig. 5. Identification results of SVM classification: (a)–(d) are physical images of Junshan Yinzhen, Wuxi White Tea, Xinyang Maojian and Lu'an Guapian. (e)–(h) Corresponding pixelwise identification results of classification.

Compared with the physical images of tea, the classification results were basically consistent with category truth values. The category classification accuracy was higher than 85%, the overall classification accuracy was 90.3%, and the kappa coefficient reached 0.87. However, mixed pixels appear at edges, and some incorrect classifications of some tea samples occur for the following reasons: 1) influences by tea-background mixed pixels or tea shieldin, 2) different postures of tea at imaging bring different reflectances ("different spectra for the same object," and 3) low chlorophyll content of tea decreases the difference among different types of tea. Generally, some differences emerge in these influences. However, the feasibility of hyperspectral images in tea identification cannot be rejected.

Table 2. Full-image statistics of tea classification accuracy

Kinds of tea		Pixel classification results (unit: pixels)				Classification accuracy (%)		
		Junshan Yinzhen	Wuxi White Tea	Xinyang Maojian	Lu'an Guapian	Category accuracy	Overall accuracy	Kappa coefficient
Category truth-value	Junshan Yinzhen	17242	1756	80	19	90.3%	90.3%	0.87
	Wuxi White Tea	1044	14806	888	79	88.0%		
	Xinyang Maojian	612	1608	16382	526	85.6%		
	Lu'an Guapian	452	144	493	23383	95.6%		

5. Conclusions

Category identification and grade classification of tea have great practical significance. Texture features and spectral features of different tea categories were extracted on the basis of hyperspectral images. Some tea identification models were built by combining the SVM model, and their accuracy values were evaluated. The following conclusions can be drawn:

(1) Compared with tea identification and classification methods based on texture features or spectral features only, the method integrating texture and spectral features achieves better classification accuracy. In particular, the overall accuracy reaches 94.3%. This outcome proves that integrating spectral and texture features can offset the influences of having different spectra for the same object to some extent.

(2) The classification model based on spectral and texture features shows the best identification effect in the four kinds of tea. The category identification accuracy, overall accuracy, and kappa coefficient are >85%, 90.3%, and 9.87, respectively. This result demonstrates that the model is feasible for identifying tea and can provide full category distribution graphs of tea.

Compared with sample-centered studies, an identification model is built considering the spectra, texture features, and hyperspectral images of tea. Then, the full category distribution graphs are provided. The conclusions of this study can provide theoretical and technological support for the rapid identification of tea. Moreover, the research results are applicable to tea detection or relevant food production enterprises. This study not only has important theoretical significance but also has favorable economic and social application prospects as well as important social and economic value. Future studies can be initiated to distinguish additional tea categories by combining spectral and image spatial features, detect and improve the stability of models, and guide authenticity identification and grade classification of tea in practical production.

Acknowledgements

This work was supported by Key Scientific Research Projects of Colleges and Universities in Henan Province (No. 21A420003, No.23A420001), Project of Science and Technology of Henan Province (No.232102321104) and General Projects of Education Science Planning in Henan Province (No.2022YB0327).

References

[1] Y. L. Hu. "The 13th Five Year Plan: the big opening of China's food safety strategy," *China Food Drug Admin. Mag.*, no.3, pp.13-14, Mar. 2017.

[2] J. H. Ma, L. X. Ji, and Q. G. Wei, "Identification technology researchof tea image levels based on multi-agent," *Comput. Simulat.*, vol.29, no.7, pp. 297-299, Jul. 2012.

[3] J. W. Zhao, Q. S. Chen, and H. Lin, "*Modern imaging technology and its application in food and agricultural product testing*," Beijing, China:Mechanical Industry Press,2011.

[4] G. K. Naganathan, L. M. Grimes, J. Subbiah, C. R. Calkins, A. Samal, and G. E. Meyer, "Visible/near-infrared hyperspectral imaging for beef tenderness prediction," *Comput. Electron. Agr.*, vol.64, no. 2, pp. 225-233, Dec. 2008.

[5] P. Talens, L. Mora, N. Morsy, D. F. Barbin, G. ElMasry, and D.W. Sun, "Prediction of water and protein contents and quality classification of Spanish cooked ham using NIR hyperspectral imaging," *J. Food Eng*., vol. 117, no. 3, pp. 272-280, Aug.2013.

[6] Z. Q. Liu, T. J. Zhou, D. H. Fu, and H. Peng, "Study on image feature extraction of fresh tea based on color and shape and its application in tea variety recognition," *Jiangsu Agr. Sci.*, vol. 49, no. 12, pp. 168-172, Jun. 2021.

[7] A. Laborde, F. Puig-castellví, D. J. Bouveresse, L. Eveleigh, C. Cordella, and B. Jaillais, "Detection of chocolate powder adulteration with peanut using near-infrared hyperspectral imaging and Multivariate Curve Resolution," *Food Control*, vol.119, Jan. 2021, Art. no.107454.

[8] G. Kos, *et al*, "A novel chemometric classification for FTIR spectra of mycotoxin-contaminated maize and peanuts at regulatory limits," *Food Addit. Contam.*, vol.33, no.10, pp. 1596-1607, Aug. 2016.

[9] H. Y. Fu, *et al*, "Predicting mildew contamination and Shelf-Life of Sunflower Seeds and Soybeans by Fourier Transform Near-Infrared Spectroscopy and Chemometric Data Analysis," *Food Anal. Method*, vol.10, no.5, pp. 1597-1608, May. 2017.

[10] Y. Huang, L. Wang, H. O. Guan, F. Zuo, and L. L. Qian, "Nondestructive detection method of mung bean origin based on optimized NIR spectral wavenumber," *Spectrosc. Spect. Anal.*, vol.41, no. 04, pp. 1188-1193, Apr. 2021.

[11] L. Chen, H. Zhang, B. C. Zhang, and L. X. Fang, "Rapid identification of original place of honeysuckle flowers based on near infrared technology," *Qual. Saf. Agr. Prod.*, no.4, pp. 41-44, Aug. 2019.

[12] L. X. Liu, D. He, M. Z. Li, X. Liu, and J. L. Qu, "Identification of Xinjiang Jujube varieties based on hyperspectral technique and machine learning," *Chin. J. Lasers*, vol.47, no.11, pp. 291-298, Jul. 2020.

[13] P. Li, *et al*, "Nondestructive identification of green tea based on near infrared spectroscopy and chemometric methods," *Spectrosc. Spect. Anal.*, vol.39, no.8, pp. 2584-2589, Aug. 2019.

[14] J. L. Zhang, "Tea image recognition based on K-Means and SVM coupling algorithm," *J. Quanzhou Norm. Univ.*, vol.34, no.6, pp. 48-54, Dec. 2016.

[15] C. Chaitra and K. V. Suresh, "Identification and evaluation of technology for detection of aflatoxin contaminated peanut," *Commun. Appl. Electron.*, vol.4, no. 5, pp. 46-50, Feb. 2016.

[16] D. J. Liu, X. F. Ning, Z. M. Li, D. X. Yang, H. Li, and L. X. Gao, "Discriminating and elimination of damaged soybean seeds based on image characteristics," *J. Stored Prod. Res.*, vol. 60, pp. 67-74, Jan.2015.

[17] Y. Wang, J. Hu, Y. K. Shao, Z. G. Yang, and J. Lv, "A study on the methods of image segmentation for tea leaf sprouts," *J. Huangshan Univ.*, vol. 17, no. 3, pp. 14-16, Jun. 2015.

[18] A. Fazari, *et a*l, "Application of deep convolutional neural networks for the detection of anthracnose in olives using VIS/NIR hyperspectral images," *Comput. Electron. Agr.*, vol.187, Jun. 2021, Art. no.106252.

[19] B. Lu, J. Sun, N. Yang, X. H. Wu, and X. Zhou, "Prediction of tea diseases based on fluorescence transmission spectrum and texture of hyperspectral image," *Spectrosc. Spect. Anal.*, vol.39, no.8, pp. 2515-2521, Aug. 2019.

[20] Y. J. Wang, *et al*, "NIR hyperspectral imaging coupled with chemometrics for nondestructive assessment of phosphorus and potassium contents in tea leaves," *Infrared Phys. Techn.*, vol.108, Aug. 2020, Art. no. 103365.

[21] R. Sonobe, Y. Hirono, and Y. Oia, "Quantifying chlorophyll-a and b content in tea leaves using hyperspectral reflectance and deep learning," *Remote Sens. Lett.*, vol.11, no.10, pp. 933-942, Jul. 2020.

[22] C. W. Xiong, *et al*, "Non-destructive determination of total polyphenols content and classification of storage periods of Iron Buddha tea using multispectral imaging system," *Food Chem.*, vol.176: pp. 130-136, Jun. 2015.

[23] Y. Q. Zhong, "A method of tibetan tea nondestructive quality inspection based on hyperspectral imagine," M.S. thesis, Coll. Mech. Electr. Eng., *Sichuan Agr. Univ.*, Ya'an, Sichuan, China, 2021.

[24] X. Ge, "Study on tea variety classification and adulteration degree detection based on hyperspectral image technology," M.S. thesis, Sch. Electr. Inf. Eng., *Jiangsu Univ.*, Zhenjiang, Jiangsu, China, 2020.

[25] T. Kelman, J. Ren, and S. Marshall, "Effective classification of Chinese tea samples in hyperspectral imaging," *Artif. Intell. Res.*, vol.2, no.4, pp. 87-91, Oct. 2013.

[26] W. Wang, G. W. Heitschmidt, W. R. Windham, P. Feldner, X. Z. Ni, and X. Chu, "Feasibility of Detecting Aflatoxin B1, on Inoculated Maize Kernels Surface using Vis/NIR Hyperspectral Imaging," *J. Food Sci.*, vol.80, no.1, pp. 116-122, Dec.2014.

[27] J. D. Rabanera, J. D. Guzman, and K. F. Yaptenco, "Rapid and Nondestructive measurement of moisture content of peanut (Arachis hypogaea L.) kernel using a near-infrared hyperspectral imaging technique," *J. Food Meas. Charact.*, vol.15, no.4, pp. 3069-3078, Aug. 2021.

[28] X. J. Qiao, J. B. Jiang, X. T. Qi, H. Q. Guo, and D. S. Yuan, "Utilization of spectral-spatial characteristics in shortwave infrared hyperspectral images to classify and identify fungi-contaminated peanuts," *Food Chem.*, vol.220, pp. 393-399, Apr.2017.

[29] T. Singh, N. M. Garg, and S. R. S. Iyengar, "Nondestructive identification of barley seeds variety using near-infrared hyperspectral imaging coupled with convolutional neural network," *J. Food Process Eng.*, vol.44, no. 10, Oct. 2021, Art. no.e13821.

[30] D. Wu and D. W. Sun, "Advanced applications of hyperspectral imaging technology for food quality and safety ananlysis and assessment: A review-Part I:Fundamentals," *Innov. Food Sci. Emerg.*, vol.19, pp. 1-14, Jul. 2013.

[31] K. J. Wang and Q. C. Guo, "Image smoothing based on the mean-shift algorithm," *J. Harbin Eng. Univ.*, vol.132, no. 11, pp. 1228-1235, Nov. 2007.

[32] A. Agrahari and R. Ghosh, "Multioriented text detection in natural scene images based on the intersection of MSER with the locally binarized image," *Procedia Comput. Sc.*, vol.171, pp. 322-330, Apr. 2020.

[33] Y. Zhang, C. Z. Ma, P. Yang, and X. M.Wang, "Face feature extraction algorithim based on wavelet transform and improved principal component analysis," *J. Jilin Univ.(Sci. E.)*, vol.59, no.06, pp. 1499-1503, Nov. 2021.

[34] F. Utaminingrum, S. J. A. Sarosa, C. Karim, F. Gapsari, and R. C. Wihandika, "The combination of gray level co-occurrence matrix and back propagation neural network for classifying stairs descent and floor," *ICT Express*, vol.8, no.1, pp. 151-160, Mar. 2022.

[35] R. Lalit and R. K. Purwar, "Crowd abnormality detection using optical flow and GLCM-based texture features," *J. Inf. Technol. Res.*, vol.15, no.1, pp. 1-15, Jun. 2022.

[36] Y. F. Long, W. Y. Qiao, and J. Sun, "Change detection of remote sensing image in Datun Mining area based on support vector machine," *Geomat. Spat. Inform. Technol.*, vol.43, no.12, pp. 107-110, Dec. 2020.

[37] S. R. Ai, R. M. Wu, Y. H. Wu, and L. Y. Yan, "Identification of geographical origins of lushan mist tea by hyperspectral imaging technology," *Acta Agr. Univ. Jiangxiensis*, no.02, pp. 428-433, Apr. 2014.

[38] Y. D. Hu, J. X. Jiang, and X. Dong, "A short-term power load forecasting method based on combining clustering and SVM parameter optimization," *Electric Power ICT*, vol.20, no.5, pp. 54-60, May. 2022.